



Green Synthesis of Copper Oxide Nanoparticles Using *Alhagi maurorum* AS Anti-Enzymatic Agent Against *Klebsiella pneumoniae* from RCU Patients

Marwa Amin Al-Rawi^{1*}, Mohammed Ameen Ahmed Al-Rawi², Labeeb A. Alzubaidi³, Bareq N. Al-Nuaimi¹,
Nada H. A. Al-Mudallal¹

¹ Department of Microbiology, College of Medicine, Al-Iraqia University, Baghdad 10001, Iraq

² Neurosurgery Teaching Hospital, Baghdad 10001, Iraq

³ Research & Technology Center of Environment, Water & Renewable Energy/Scientific Research Commission, Baghdad 10001, Iraq

Corresponding Author Email: marwa.a.ahmed@aliraqia.edu.iq

Copyright: ©2025 The authors. This article is published by IIETA and is licensed under the CC BY 4.0 license (<http://creativecommons.org/licenses/by/4.0/>).

<https://doi.org/10.18280/ijdne.200518>

ABSTRACT

Received: 8 March 2025

Revised: 20 April 2025

Accepted: 24 April 2025

Available online: 31 May 2025

Keywords:

copper oxide nanoparticles, *Alhagi maurorum*, anti-enzymatic, *Klebsiella pneumoniae*, respiratory infections, RCU

Multidrug-resistant bacteria often produce enzymes that are closely associated with virulence and pathogenicity. To investigate the anti-enzymatic activity of copper oxide nanoparticles (CuONPs), synthesized using *Alhagi maurorum* plant extract, against *Klebsiella pneumoniae*. A total of 100 sputum samples were collected from patients admitted to the respiratory care unit (RCU). The bacterial isolates were identified by culturing on MacConkey agar and blood agar, followed by biochemical confirmation using the VITEK-2 system. *Alhagi maurorum* was collected, ground, and extracted for its phytochemical constituents. CuONPs were synthesized and prepared using the *Alhagi maurorum* extract as a reducing and capping agent. Characterization was performed using Fourier transform infrared (FTIR) spectroscopy, zeta potential analysis, atomic force microscopy (AFM), and transmission electron microscopy (TEM). Enzymatic activity was assessed using the agar well diffusion method. The characterization results confirmed the successful synthesis of *Alhagi maurorum*-mediated CuONPs with high purity and a crystalline structure. FTIR analysis revealed strong interactions between phytochemicals from *Alhagi maurorum* and the CuONPs. A zeta potential value of +48.15 mV indicated excellent colloidal stability of the synthesized nanoparticles. While the *Alhagi maurorum* extract alone showed minimal anti-enzymatic activity, CuONPs at a 20% concentration exhibited significant activity, with an inhibition zone of 45.7 ± 3.3 mm ($P = 0.0001$). The combination of *Alhagi maurorum* extract and CuONPs at 20% concentration also showed significant anti-enzymatic activity, with an inhibition zone of 41.9 ± 3.7 mm ($P = 0.0001$). The anti-enzymatic properties of CuONPs and *Alhagi maurorum*-mediated CuONPs (AH.CuONPs) represent a promising strategy for mitigating the virulence of *Klebsiella pneumoniae*.

1. INTRODUCTION

Multidrug-resistant (MDR) bacteria have emerged as a significant global health concern, particularly in the context of respiratory tract infections [1, 2]. The most frequently isolated bacteria in the respiratory care unit (RCU) patients include *Pseudomonas aeruginosa*, *Staphylococcus aureus*, *Acinetobacter* spp., and *Klebsiella pneumoniae*. Unfortunately, these pathogens have become increasingly difficult to treat due to their acquired resistance to commonly used antibiotics [3-5]. The pathogenicity and antibiotic resistance of many respiratory tract bacteria require the production of various enzymes [6]. Enzymes such as β -lactamases, proteases, and lipases play a key role in mediating bacterial dissemination and survival within the host [7]. Bacterial proteases play vital functions in cell physiology, replication, and survival. Extracellular proteases are responsible for the destruction of host tissue and the degradation of host defense proteins,

including immunoglobulin A (IgA) [8]. This highlights the urgent need to develop novel strategies to combat infections caused by resistant pathogens [9].

Metal oxide nanoparticles (NPs), including CuONPs, have emerged as promising antimicrobial agents due to their multiple mechanisms of action, such as reactive oxygen species (ROS) generation, disruption of microbial membranes, and interference with the action of some important enzymes critical for their survival [10]. Some metal oxide nanoparticles present properties involving high biocompatibility and a great surface area available for interaction with biotic materials [11].

One rapidly expanding area of interest is the green synthesis of nanoparticles using plant extracts, which have a much lower ecological and budgetary cost than other classical chemical approaches [12]. The green synthesis of nanoparticles is attracting considerable interest as an environmentally acceptable and sustainable alternative to traditional chemical and physical processes. This method reduces the usage of toxic

chemicals, decreases energy consumption, and enhances the biocompatibility of nanoparticles, making it particularly suitable for biomedical and environmental applications. Green nanoparticles possess distinctive physicochemical characteristics, including higher surface area, reactivity, and targeted efficacy against multidrug-resistant infections, hence boosting their capacity to compromise multidrug-resistant bacterial membranes. They may be integrated with current antibiotics to overcome resistance processes, therefore enhancing therapeutic efficacy. Moreover, green production improves the biocompatibility of nanoparticles, rendering them safer for medicinal uses [13, 14].

Plants continue to be a significant source of several chemicals that support better human health and potential raw materials for nanoparticle synthesis. One promising plant is *Alhagi maurorum* due to its presence of antimicrobial and antioxidant compounds [15].

Alhagi maurorum is a member of the Fabaceae family and grows widely in sandy soils. The plant blooms between May and July and can grow up to two meters in height. The big leguminous plant has sharp thorns on its greyish-green leaves and roots that reach up to 6 feet deep in the earth [16]. *Alhagi maurorum* has demonstrated many preventative qualities, particularly its potent antibacterial and antioxidant effects. Its raw extracts and chemical constituents have been the subject of much research [17].

Studies have shown that nanoparticles can interfere with enzymatic activity, thereby reducing the pathogenicity of various bacterial strains [18].

The present study investigated the anti-enzymatic activity of CuONPs synthesized using *Alhagi maurorum* extract against bacterial strains isolated and identified from sputum samples of patients in respiratory care units (RCUs). This approach offers a sustainable and effective strategy for treating infections caused by antibiotic-resistant pathogens.

2. MATERIALS AND METHODS

2.1 Collection of sputum samples

The present study was conducted in the period between November 2023 to July 2024. One hundred (100) sputum samples were collected from 38 females, 53 males, and 9 children's patients who were admitted to the RCU in Al-Yarmouk Teaching Hospital and Neurosurgery Teaching Hospital, respectively. Samples were aseptically collected in sterile vials and transported to the laboratory. The study received ethical clearance from the Ethical Committee of Al-Iraqi University/College of Medicine/Microbiology Department.

2.2 Isolation of bacteria and determination of antibiotic resistance

The sputum samples were cultured on blood, chocolate, and MacConkey agars to isolate the bacterial pathogens of the respiratory tract. Subculturing was performed onto freshly prepared media to purify the mixed cultures. The isolates were identified using standard microbiological techniques, such as Gram staining and biochemical tests (Urease and Simmons citrate) [19]. The antibiotic resistance and diagnostic bacteria of the isolates were determined by using the VITK-2 system following the manufacturer's instructions.

2.3 Detection of protease-producing bacterial isolates

The protease enzyme activity was determined using a skim milk agar medium. To prepare skim milk agar, 51.5 grams of nutrient agar was suspended in 1 liter of distilled water and boiled until completely dissolution. Sterilization was done by autoclaving the medium at 121°C for 15 minutes. It was allowed to cool to 45°C, and 5 mL skim milk was added and then dispensed into sterile Petri dishes [20]. Protease production was detected in the bacterial isolates by measuring the clearance zone diameter in skim milk agar. After preparing the milk skim agar, a cork borer with a diameter of 0.6 mm was used to make four wells in each Petri dish. The bacterial suspension was adjusted with McFarland solution 1.5×10^8 and dispensed into each well to detect which isolates produced protease. The bacterial suspension that grew on nutrient broth before one day of incubation at 37°C was diluted with sterile normal saline and compared with the McFarland Standard (1.5×10^8) [21].

2.4 Collection and extraction methodologies of *Alhagi maurorum* plants

Fresh *Alhagi maurorum* plants were collected from their natural habitat in Abo Gareeb, Baghdad by a botanist. The plant material was washed with distilled water, air-dried, and ground into a fine powder to extract compounds [15]. The air-dried ground *Alhagi maurorum* plant material, weighted 100 grams for each sample, was extracted with the aqueous methanol (methanol: water, 80% v/v) 500 mL solvent for 8 hours under Soxhlet on a water bath in separate experiments [22]. The extracts were concentrated and freed of solvent under reduced pressure at 45°C using a rotary evaporator. The dried crude concentrated extracts were weighed to calculate the yield and stored in a refrigerator at 4°C until used.

2.5 Synthesis of copper nanoparticles

Polyvinyl alcohol-PVA and Vitamin C (1%) were added to freshly prepared 0.2 M copper nitrate solution in a ratio of 1:1:3, respectively. Accompanied by constant stirring, the solution was heated for 4 hours at 55°C until a colour change was observed with some modification. The fully reduced solution was centrifuged for 15 minutes at room temperature, 5000 rpm, washed, and stored at 4°C until further use [23-25].

2.6 Preparation of *Alhagi maurorum*-copper oxide nanoparticles

To 200 mL of distilled water, the powdered plant materials were added and heated at 60°C for 30 minutes. The resultant heated mixture was filtered using Whatman No. 1 filter paper. The obtained filtrate was stored at 4°C and used later for the synthesis of nanoparticles [18]. A concentration of 0.1 M aqueous solution of copper sulphate (CuSO_4) was prepared. *Alhagi maurorum* extract was added dropwise to copper sulphate (CuSO_4) solution under stirring conditions. The reaction mixture was kept at 70°C for 2 hours; due to time, colouring changes indicated the development of *Alhagi maurorum*-copper oxide nanoparticles (AH.CuONPs). Centrifugation of the solution was performed at 10,000 rpm for 20 minutes, followed by washing with distilled water and ethanol and drying at 60°C for 12 hours for further characterization [11].

2.7 Characterization of *Alhagi maurorum*-copper oxide nanoparticles

The synthesized nanoparticles were characterized using Fourier transform infrared (FTIR), X-ray diffraction (XRD) analysis, zeta potential analyses, Atomic Force Microscopy (AFM), and transmission electron microscopy (TEM).

FTIR examination of the samples was performed in the range of 400-4000 cm⁻¹. FTIR analysis was used to detect the functional groups potentially responsible for the reduction of copper nanoparticles from *Alhagi maurorum* extract and their stabilization. The diffraction peaks (XRD) in both CuONPs and *Alhagi maurorum*-stabilized CuONPs patterns revealed valuable information about the crystalline structure of the synthesized nanoparticles. AFM analysis is a technique used to map surfaces with nano and even micron dimensions and to measure the flexibility of nanoparticles. Transmission electron microscopy was used to evaluate the AH-CuONPs at different magnifications to ascertain the nanoparticle sizes.

2.8 Determination of the enzymatic activity of test solutions

The determination of anti-enzymatic activity of CuONPs, AHCuONPs, and *A. maurorum* plant extract was done using the agar-well diffusion method. The bacterial cultures were incubated with three different concentrations, 10%, 20%, and 40%, of the tested solutions [18]. An amount of the respective tested solution was added to a bacterial suspension in a sterilized container; subsequently, an aliquot of 0.1 ml of that mixture was introduced into separate wells on nutrient agar. The positive control had 0.1 ml of bacterial suspension adjusted to McFarland standard without any addition, and the negative control consisted of 0.1 ml of normal saline. One well was treated with *A. maurorum* extract mixed with the bacterial suspension, which was adjusted to the McFarland standard, and in another well, an *A. maurorum*-CuONPs mixture with bacterial suspension adjusted to the McFarland standard was added. A separate well was prepared with 0.1 ml of CuONPs mixed with bacterial suspension, also adjusted to the McFarland standard (to measure the concentration of bacteria). The nutrient agar plates were incubated at 37°C for

24 hours to allow bacterial growth and evaluate the anti-enzymatic activity of the test solutions.

2.9 Statistical analysis

Triplicate sets of all experiments were performed, and the data obtained were subjected to a statistical package (IBM SPSS, Chicago, IL, USA; version 29). Values obtained were expressed as mean ± standard error of mean (SEM). For testing significant differences in quantitative data, a Student's T-test comparing two independent means or more than two independent means through ANOVA was employed. A p-value of ≤ 0.05 was considered statistically significant.

3. RESULTS

3.1 Bacterial isolation, identification, and antibiotic resistance

One hundred (100) sputum samples were cultivated on blood agar, MacConkey agar, and chocolate agar to identify the bacterial species. The isolates underwent many biochemical tests, including the triple sugar iron (TSI) assay, urea hydrolysis, and Simmons' citrate. The results of biochemical tests are demonstrated in Table 1. Gram-stained bacterial smears were examined under a microscope to show the variations in cell shapes. Results revealed that *Acinetobacter baumannii* and *Klebsiella pneumoniae* were the most isolated bacteria in the RCU sputum samples, 34 (34%) and 28 (28%) isolates, respectively. *Klebsiella pneumoniae* presented in ten (10%) of the isolates (Figure 1). Other bacterial isolates include one isolate of *Proteus mirabilis*, one isolate of *Staphylococcus aureus*, one isolate of *Pseudomonas aeruginosa*, and three samples of normal flora. Forty-three of the 100 sputum samples showed no signs of bacterial development (Table 2). The VITEK-2 system was used to further validate identification. All samples were found resistant to Amikacin, Gentamicin, Tobramycin, Ciprofloxacin, pefloxacin, Minocycline, Colistin, Rifampicin, Trimethoprim, Ceftazidime, Cefepime, Aztreonam, Imipenem, and Meropenem.

Table 1. Biochemical tests of gram-negative bacterial isolates

| Bacterial Isolates | <i>K. pneumonia</i> | <i>A. baumannii</i> | <i>P. mirabilis</i> | <i>P. aeruginosa</i> |
|----------------------|---------------------|---------------------|---------------------|----------------------|
| Gram Stain | - | - | - | - |
| Citrate | + | + | + | + |
| Lactose fermentation | + | + | - | - |
| Indole | - | - | - | - |
| (TSI) | A/A+ - | K/K | K/A++ | K/K - |
| Urease | - | - | + | - |
| Oxidase | - | - | - | + |
| Catalase | + | + | + | + |

Table 2. Percentage occurrence of bacterial isolates from sputum samples

| Bacterial Isolate | Frequency of Occurrence | Percentage of Occurrence |
|---------------------------|-------------------------|--------------------------|
| <i>Acinetobacter</i> spp. | 27 | 47.4 |
| <i>A. baumannii</i> | 7 | 12.3 |
| <i>Klebsiella</i> spp. | 18 | 14.0 |
| <i>K. pneumonia</i> | 10 | 17.4 |
| <i>P. mirabilis</i> | 1 | 1.8 |
| <i>S. aureus</i> | 1 | 1.8 |
| Normal flora | 3 | 5.3 |
| Total | 57 | 100.0 |

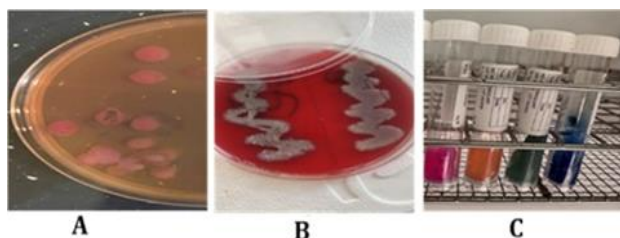


Figure 1. Cultural and biochemical tests for bacterial isolates. (A) *Klebsiella* species on MacConkey agar; (B) *Klebsiella* on blood agar; (C) Urease and Simmons citrate biochemical assays used for identifying *Klebsiella* species

3.2 Production of the protease enzyme by *Klebsiella pneumoniae*



Figure 2. Protease production by *Klebsiella pneumoniae*

Klebsiella pneumoniae was selected from the isolated species to reveal the enzymatic activity of protease production. The ability of this bacterium to produce an enzyme was

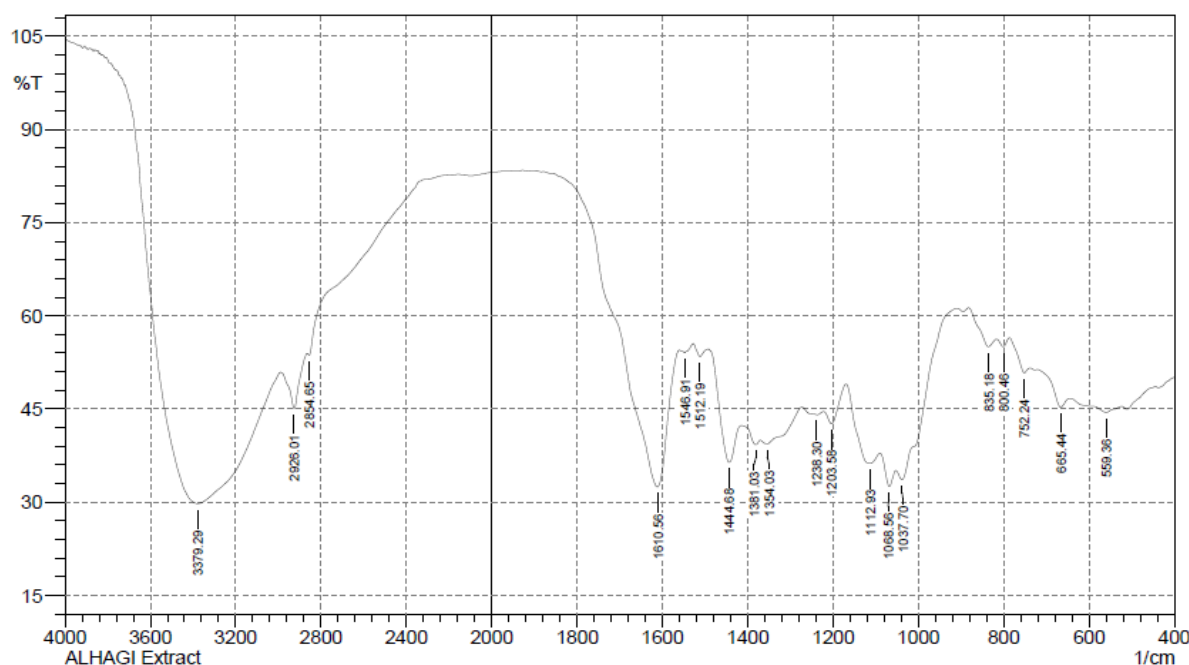
assessed using a protease enzyme assay for each of the *Klebsiella pneumoniae* isolates. Further analysis revealed protease production in four (4/10) *Klebsiella pneumoniae* isolates. Clear zones surrounding bacterial colonies were observed, confirming protease production (Figure 2).

3.3 Characterization of *Alhagi maurorum* plant extract and copper oxide nanoparticles

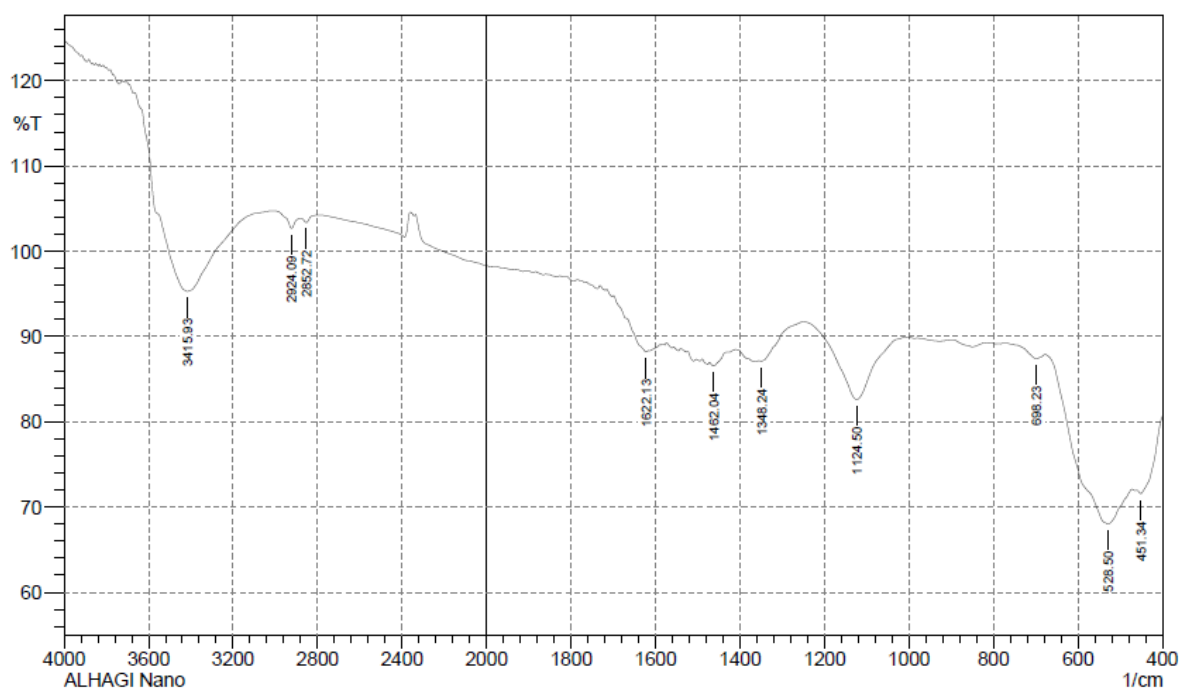
3.3.1 Functional group determination: Fourier transform infrared analysis (FTIR)

Results of the variations in the chemical bonds characteristic of the peaks responsible for the stretching vibrations of the $-OH$ groups were referred to the phenolic compounds present in the FTIR spectra of the plant extract (3379.29 cm^{-1}) and copper nanoparticles from *Alhagi maurorum* extract at (3415.93 cm^{-1}), but the disappearance of other peaks when examining the FTIR of the same sample, which are 1037.70 , 1068.56 , 1203.58 , 1238.30 , 1354.03 and 1512.19 cm^{-1} indicate the extension of C-N stretch, C-H rock, N-O symmetric stretch, and the disappearance of the peaks from 753.24 - 835.19 cm^{-1} (aromatic cyclic compounds). Peaks at 528.50 cm^{-1} and 509.21 cm^{-1} were observed for copper nanoparticles synthesized using *Alhagi maurorum* extract and for chemically synthesized copper nanoparticles, respectively, indicating the presence of copper. These findings suggest a successful interaction between the bioactive compounds in the plant extract and the nanoparticle matrix. Additionally, the broad O-H stretching band was slightly shifted, implying stabilization of the nanoparticles through hydrogen bonding or other surface interactions. Prominent peaks around 1600 cm^{-1} were also retained, confirming the presence of aromatic compounds, as illustrated in Figure 3.

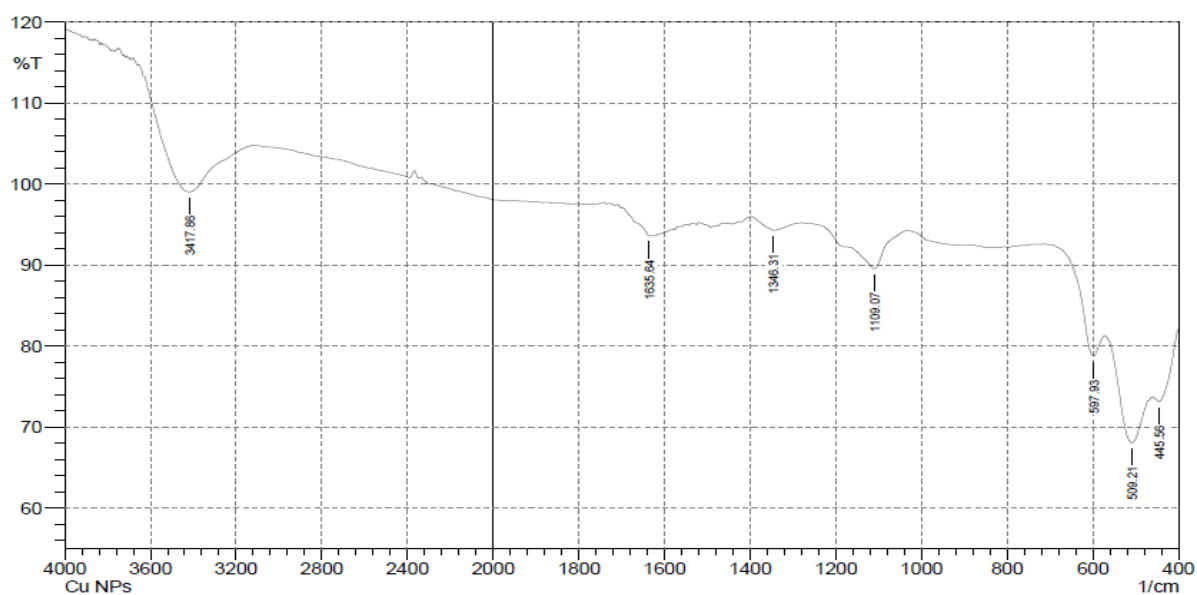
SHIMADZU



(A)



(B)



(C)

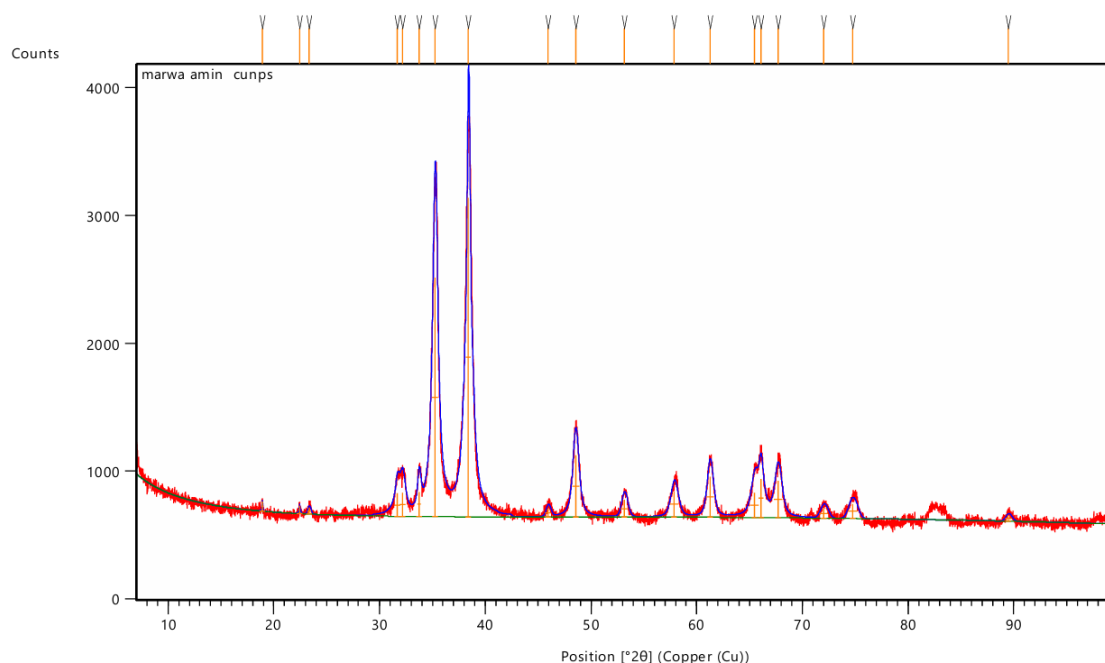
Figure 3. (A) FTIR analysis of *Alhagi maurorum* extract, (B) *Alhagi maurorum* extract-copper oxide nanoparticles, (C) copper oxide nanoparticles

3.3.2 X-ray diffraction (XRD) analysis of nanoparticles: crystalline structure

The XRD pattern of CuONPs exhibited sharp and well-defined peaks at specific 2θ values, corresponding to characteristic planes of copper oxide, CuO (Figure 4(A)). These peaks confirm the formation of highly crystalline monoclinic CuO, indexed by the Joint Committee on Powder Diffraction Standards (JCPDS). In the case of *Alhagi maurorum*-stabilized CuONPs, the XRD pattern retains the characteristic peaks of CuO observed in Figure 4(A), showing that the crystallinity of the nanoparticles is preserved after stabilization. However, some extra peaks of lower intensity

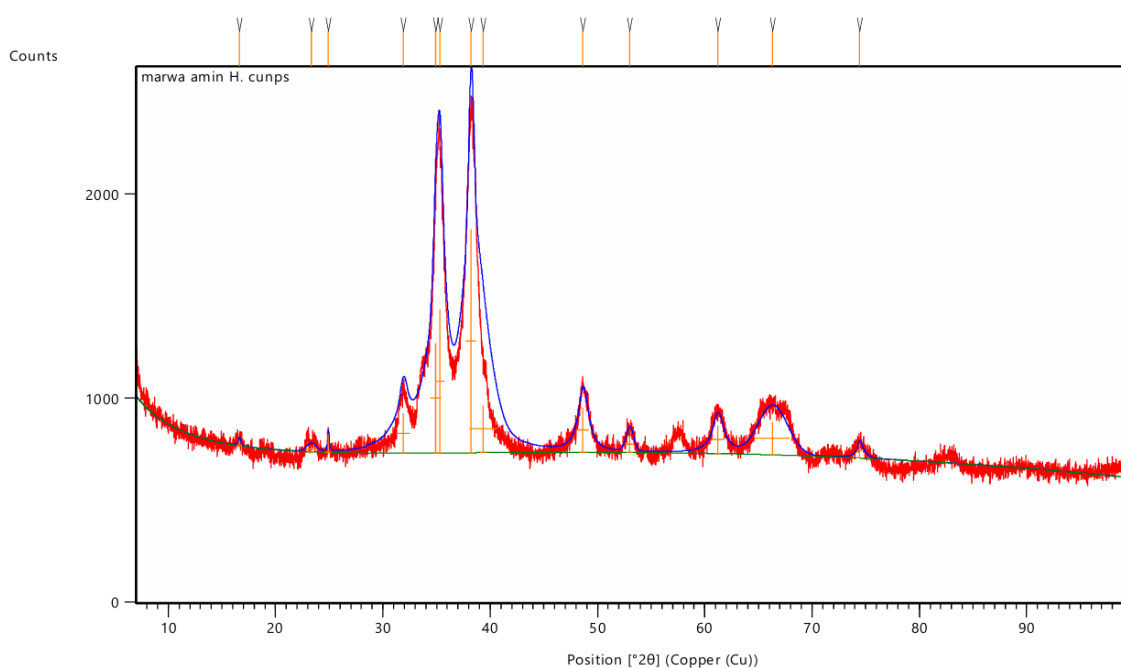
were observed, which may be due to the amorphous organic components of *Alhagi maurorum* extract adsorbed on the nanoparticle surface (Figure 4(B)). The absence of any extraneous peaks in both spectra confirms the purity of the samples, which further proves that no impurities or other phases were introduced during the synthesis process. These results substantiate the successful synthesis of crystalline CuONPs and their stabilization by *Alhagi maurorum* extract. The consistent crystallinity and absence of impurity phases further validate the efficiency of *Alhagi maurorum* as a bio-template for eco-friendly nanoparticle synthesis.

Main Graphics, Analyze View: (Bookmark 2)



(A)

Main Graphics, Analyze View: (Bookmark 2)



(B)

Figure 4. XRD analysis of test solutions. (A) Copper oxide nanoparticles (CuONPs), (B) *Alhagi maurorum* extract-CuONPs

3.3.3 Zeta potential analysis of nanoparticles: Surface charge and stability

The zeta potential of the synthesized nanoparticles shows that the zeta potential of *Alhagi maurorum*-CuONPs, measured at +48.15 mV, indicates good stability due to strong electrostatic repulsion (Figure 5(A)). The zeta potential of CuONPs, measured at +59.82 mV, reflects a higher degree of stability than *Alhagi maurorum*-CuONPs (Figure 5(B)). The positive zeta potential values suggest that both nanoparticles exhibit significant surface charges, which may enhance colloidal stability in dispersion.

3.3.4 Atomic Fluorescent Microscopy (AFM)

In a result of 3D copper nanoparticles with *Alhagi maurorum* extract, the shape of the nanoparticles were smooth spherical nanoparticles, 94.34 nm is high result referring to copper element and average size particles (7.892-317.3) nm; as a result, of aggregation nanoparticles because the sample drying for the analysis preparation process, with acute nanoparticles edges and high roughness period (Figure 6(A)). As a result of 3D copper nanoparticles, the shape of the nanoparticles were smooth spherical nanoparticles, 108 nm is a high result referring to copper element and average size

particles (15.67-265.5) nm; as a result, of aggregation nanoparticles because the sample drying for the analysis preparation process, with acute nanoparticles edges and high roughness period (Figure 6(B)).

3.3.5 Transmission electron microscopy (TEM)

After using TEM, results show that CuONPs are agglomerated and lack a distinct morphology (Figure 7(A) and (B)). It was discovered that AH-CuONPs had an average particle size of about 50 nm.

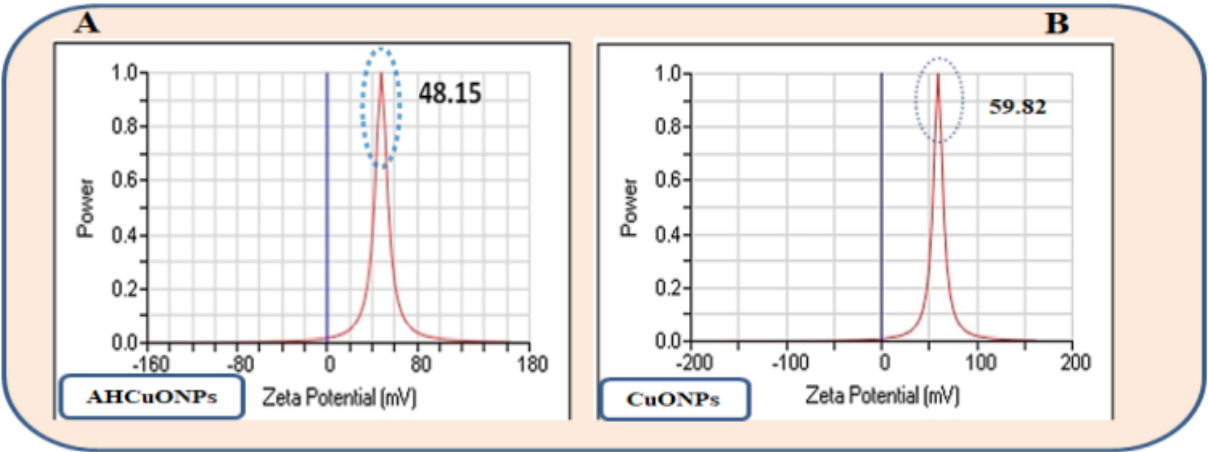


Figure 5. Zeta potential analysis. (A) *Alhagi maurorum*-copper oxide nanoparticles (AHCuONPs), (B) copper oxide nanoparticles (CuONPs)

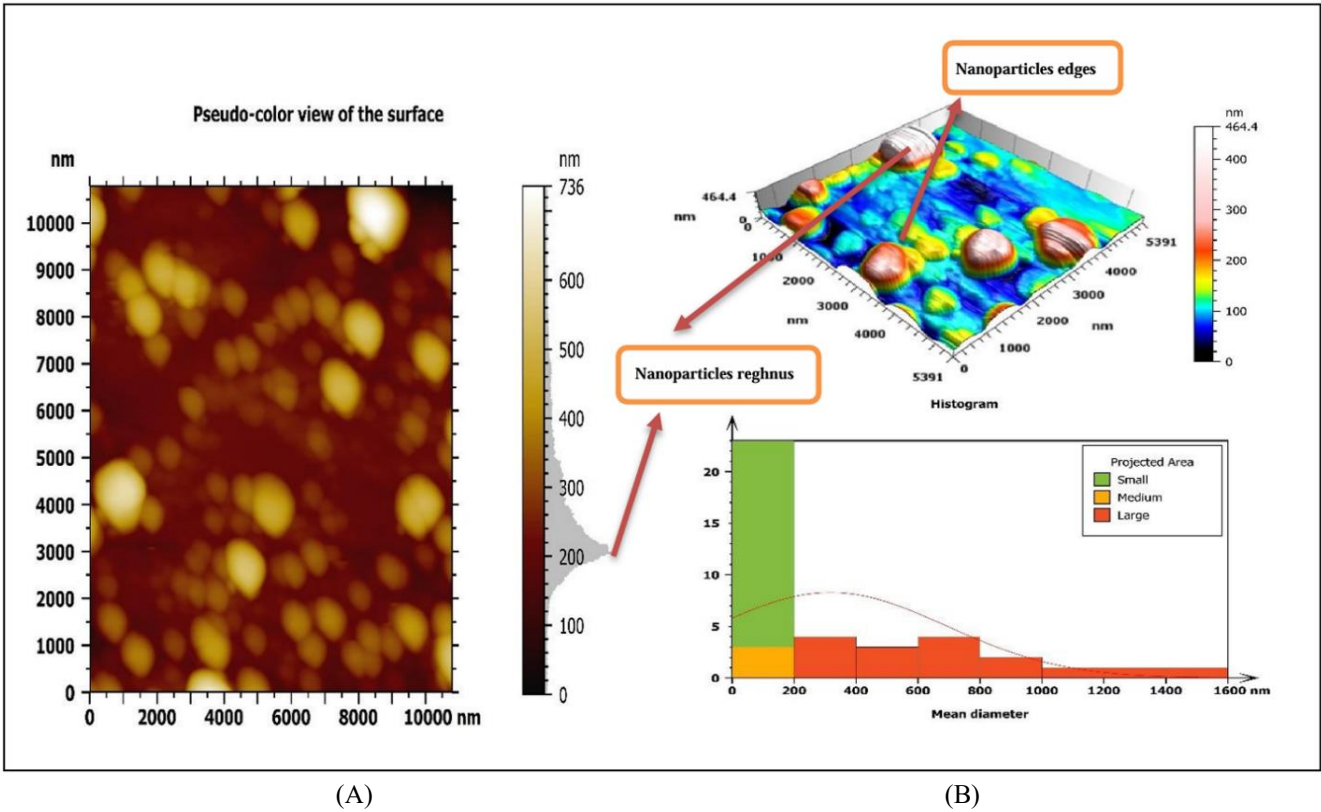


Figure 6. AFM images of (A) *Alhagi maurorum*-copper oxide nanoparticles, (B) copper oxide nanoparticles

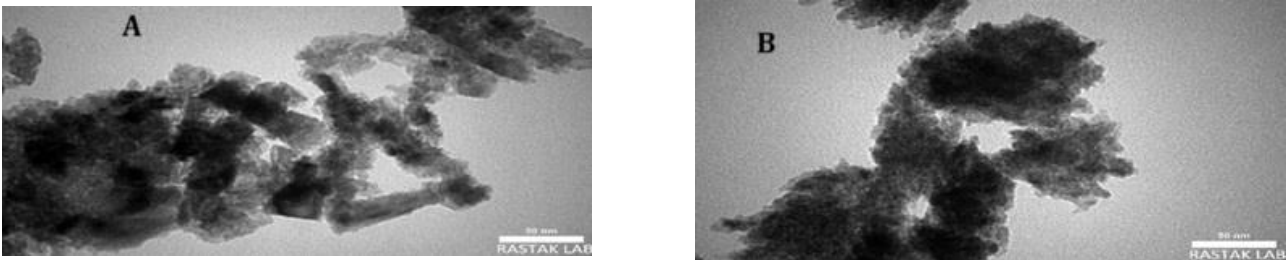


Figure 7. TEM images of (A) CuONPs, (B) AH-CuONPs

3.4 Inhibition of enzymatic activity against *Klebsiella* spp.

The effect of *Alhagi maurorum* extract, CuONPs, and a combination of *Alhagi maurorum*-CuONPs against protease-producing *Klebsiella* spp. was examined. Varying concentrations (10%, 20%, and 40%) of CuONPs, *Alhagi maurorum*-CuONPs, and *Alhagi maurorum* extract on four isolates of *Klebsiella pneumoniae*, with controls included for comparison. The results demonstrated variations in anti-enzymatic efficacy depending on the treatment type and concentration (Figure 8).

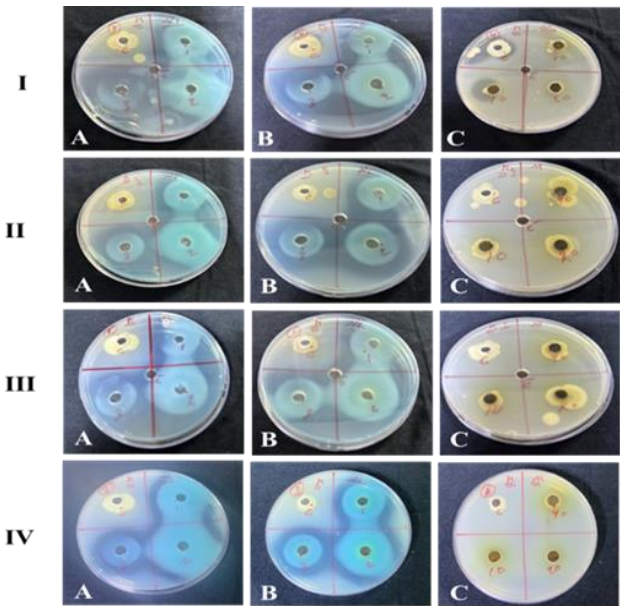


Figure 8. Anti-enzymatic activity of *Alhagi maurorum* extract-copper oxide nanoparticles against isolates of *Klebsiella* species

Alhagi maurorum plant extract alone exhibited minimal anti-enzymatic activity against protease-producing *Klebsiella*

spp. Even at higher concentrations, the inhibitory effect of *Alhagi maurorum* was negligible, suggesting that the extract's bioactive compounds alone are insufficient to significantly inhibit protease production by *Klebsiella* spp. CuONP nanoparticles alone displayed considerable anti-enzymatic activity, with inhibition increasing dose-dependent. CuONP (20%) concentration demonstrated the highest anti-enzymatic activity. The inhibition zone was 45.7±3.3 mm (Table 3). The combination of *Alhagi maurorum* and CuONPs demonstrated a significant anti-enzymatic activity with inhibition zones 38.1±3.3, 41.9±3.7, and 33.8±4.0 of 10%, 20%, and 40%, respectively. This synergistic effect is attributed to the combined action of CuONPs and the bioactive compounds in the extract, which may enhance bacterial membrane disruption or enzyme inhibition. The anti-enzymatic effect was concentration-dependent, with the most significant inhibition observed at 20% concentrations of the CuONPs and 20% concentrations of the extract-CuONPs combination (AHCuONPs) (Figure 9).

Table 3. The inhibition zones (mm) of *Klebsiella pneumoniae* after treatment by *Alhagi maurorum* extract, CuONPs, and a combination of *Alhagi maurorum*-CuONPs

| Material/ Concentration | Inhibition Zone Diameter Means (mm) | P-value Compared to Control +Bacteria |
|----------------------------|-------------------------------------------|------------------------------------------------|
| Cu 10% | 38.2±5.3 (31-48) | 0.0001* |
| Cu 20% | 45.7±3.3 (40-50) | 0.0001* |
| Cu 40% | 35.1±4.0 (29-44) | 0.001* |
| Cu+M 10% | 38.1±3.3 (33-44) | 0.0001* |
| Cu+M 20% | 41.9±3.7 (36-48) | 0.0001* |
| Cu+M 40% | 33.8±4.0 (29-42) | 0.003* |
| M only 10% | 0.0± | 0.0001* |
| M only 20% | 0.0± | 0.0001* |
| M only 40% | 0.0± | 0.0001* |
| Control+ Bacteria | 26.8±3.3 (22-32) | |
| Distilled water | 0.0± | |

P-value compared to Control + Bacteria

* Highly significant (P<0.01).

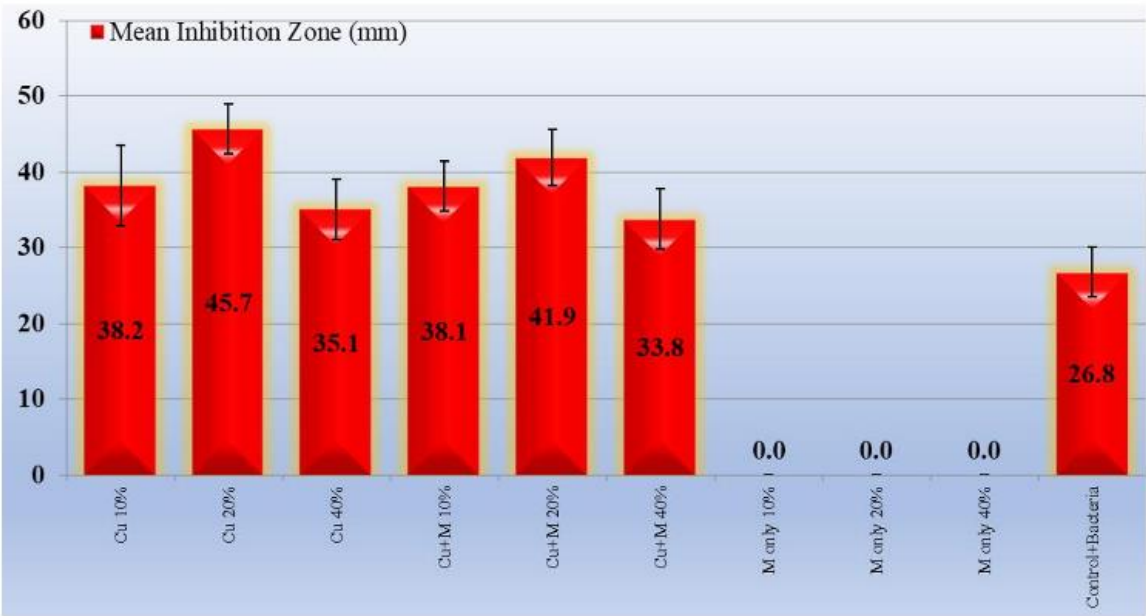


Figure 9. Anti-enzymatic activity of tested solutions against protease-producing *Klebsiella pneumoniae*

4. DISCUSSION

The increasing prevalence of MDR bacterial strains, especially in hospital settings, is a key challenge in managing respiratory tract infections. Various enzymes, including proteases, lipases, and β -lactamases, are associated with virulence, resistance, and pathogenicity of the microorganisms. *Klebsiella pneumoniae*, a Gram-negative bacterium, produces proteases that significantly impact the respiratory tract. These proteases contribute to the pathogen's virulence by breaking down host tissues and immune defences, facilitating infection and colonization [26]. In the respiratory tract, *Klebsiella* proteases can degrade mucosal barriers and immune proteins, such as immunoglobulins, impairing the host's ability to fight off the infection. This can lead to severe respiratory infections, particularly in immunocompromised individuals or those with underlying health conditions [27]. In light of these findings, this study addresses an urgent need for alternative strategies by investigating anti-enzymatic properties of the *Alhagi maurorum*-mediated copper oxide nanoparticles against one of the most important bacterial pathogens isolated from sputum samples of RCU patients, which is *Klebsiella* spp. The findings identified a synergistic interplay in the phytochemicals of *Alhagi maurorum*, together with the antimicrobial potential of CuONPs, which presents encouraging perspectives in counteracting MDR bacterial infections.

The FTIR spectra revealed functional groups in the *Alhagi maurorum* plant extract and their interaction with CuONPs. The observed O–H stretching and C=C aromatic peaks are comparable to findings by Kumar et al. [28], who identified similar functional groups in plant-extract-mediated nanoparticle synthesis. The shifts in peak positions in *A. maurorum*-CuONPs confirm successful stabilization, consistent with observations by Sharma et al. [29]. This interaction highlights the potential of *A. maurorum* phytochemicals in nanoparticle functionalization. Researchers rely on a powerful and popular analytical tool, infrared (IR) spectroscopy, when studying the biosynthesis of copper nanoparticles and the structure of copper nanoparticles alone, which depends on the vibrations of the atoms of the molecule. It is possible to qualitatively identify the types of bonds in the sample by comparing the energy of each absorption peak with the vibration frequency of the molecular component. The efficiency and accuracy of IR spectroscopy have been greatly enhanced by the advent of Fourier transform infrared (FTIR) spectroscopy, which has significantly reduced data acquisition times [30].

The XRD patterns confirmed the monoclinic crystalline structure of CuONPs, with additional amorphous peaks attributed to organic components from *A. maurorum*. Similar crystallinity was reported in a study conducted in biosynthesized CuONPs [31]. However, the findings in the present study uniquely demonstrate the retention of crystallinity post-stabilization, emphasizing the extract's efficiency as a bio-template. The zeta potential measurements indicated strong stability of *A. maurorum*-CuONPs (+48.15 mV) and CuONPs (+59.82 mV). These values are consistent with earlier studies, such as those by Pandey et al. [32], which reported high zeta potentials in green-synthesized nanoparticles. Meanwhile, *A. maurorum*-CuONPs showed slightly lower stability than CuONPs; the stability remains sufficient for practical applications, indicating the extract's

effective capping ability.

Production of protease was eminently high in a few isolates of *K. pneumoniae*, which once again upholds its relationship with bacterial adaptability and virulence. Previous findings suggest that protease production is strain-specific, which may correlate with the isolates' pathogenicity or environmental adaptability. The present findings revealed that *Klebsiella* strains possess the capacity for extracellular protease secretion, with potential implications for their pathogenicity and environmental roles.

Copper nanoparticles exhibit remarkable antibacterial properties due to their unique physical and chemical characteristics. The small size and smooth surface of CuONPs and their spherical shape work to achieve high adhesion to bacterial cells, thus causing penetration of nanoparticles into bacterial cells and preventing enzyme production. The high effectiveness of copper nanoparticles, in addition to active compounds such as phenols, alkaloids, and falcons, increases the effectiveness of the nanomaterial and reduces the toxicity of the application [33].

The significant inhibition of enzymatic activity by CuONPs and AHCuONPs highlights their dual role in antimicrobial action: direct bacterial killing and suppression of virulence factors. This anti-enzymatic activity is particularly relevant in the context of MDR pathogens, where targeting non-essential but virulence-associated enzymes can reduce bacterial fitness and resistance. The observed synergistic effects between *Alhagi maurorum* extract and CuONPs in inhibiting enzymatic activity align with findings by Chong and Shimoda [7] and Liu et al. [11], emphasizing the potential of nanoparticle-based therapies to disrupt bacterial metabolic pathways.

4.1 Comparative efficacy and clinical implications

The comparative analysis of CuONPs, *Alhagi maurorum* extract, and AHCuONPs revealed that the nanoparticles CuONPs (20%) exhibited superior anti-enzymatic properties. This enhancement likely stems from the interaction between CuONPs and *Alhagi maurorum* phytochemicals, which amplify oxidative stress and disrupt bacterial enzymatic systems. Similar synergistic interactions have been reported in studies involving plant-mediated nanoparticle synthesis [15]. The clinical implications of these findings are substantial. AHCuONPs offer a dual-action approach by directly targeting bacterial viability and virulence factors. This strategy not only reduces bacterial loads but also diminishes the likelihood of resistance development. Moreover, the green synthesis method revealed a good biocompatibility, making AHCuONPs suitable for potential therapeutic applications in respiratory infections and beyond, in addition to CuONPs alone.

4.2 Limitations and future directions

While the present study provides compelling evidence for the efficacy of AHCuONPs, several limitations warrant consideration. The molecular mechanisms underlying the observed anti-enzymatic effects require further investigation. Additionally, in vivo studies are essential to evaluate the biocompatibility, safety, and therapeutic potential of AHCuONPs. Future research should also explore the scalability of the green synthesis method and its applicability to other bacterial pathogens and enzymatic targets.

5. CONCLUSION

The anti-enzymatic activity of *Alhagi maurorum* extract, CuONPs, and a combination of *Alhagi maurorum*-CuONPs (AH.CuONPs), against protease-producing *Klebsiella* spp. was conducted in the current study.

Alhagi maurorum plant extract alone exhibited minimal anti-enzymatic activity against protease-producing *Klebsiella* spp. CuONP nanoparticles alone displayed considerable anti-enzymatic activity, with an inhibition zone of 45.7 ± 3.3 mm at 20% concentration. The combination of *Alhagi maurorum* and CuONPs demonstrated a significant anti-enzymatic activity with an inhibition zone of 41.9 ± 3.7 at 20% concentration.

The combination of CuONPs with phytochemicals derived from *Alhagi maurorum* expresses an augmented action on microorganisms through interaction in such a way that it has enhanced its potential to kill microbes synergistically via hindering virulence factors, including the protease enzyme.

The anti-enzymatic effect was concentration-dependent, with the most significant inhibition observed at 20% concentrations of the CuONPs and extract-CuONPs combination (AHCuONPs).

Future investigations should be directed toward elucidating the exact molecular mechanism for the improved anti-enzymatic properties. In *vivo* studies are also important in determining their safety, biocompatibility, and therapeutic potential.

REFERENCES

- [1] Al-Aameri, D.A., Zghair, S.A., Al-Nuaimi, B.N., Abdul-Ghani, M.N., Naman, Z.T., Fadhil, Z.J. (2024). Evaluation of susceptibility of *Candida* species to six antifungal drugs in Iraqi specimens. *Journal of Communicable Diseases*, 56(2): 53-61. <https://doi.org/10.24321/0019.5138.202432>
- [2] Al-Aameri, D., Al-Nuaimi, B.N. (2020). Mutations in ergosterol 11 gene of fluconazole resistant *Candida albicans* isolated from different clinical samples. *Malaysian Journal of Biochemistry and Molecular Biology*, 23(1): 57-61.
- [3] van Duin, D., Paterson, D.L. (2020). Multidrug-resistant bacteria in the community: An update. *Infectious Disease Clinics of North America*, 34(4): 709-722. <https://doi.org/10.1016/j.idc.2020.08.002>
- [4] Qin, S., Xiao, W., Zhou, C., Pu, Q., Deng, X., Lan, L., Liang, H., Song, X., Wu, M. (2022). *Pseudomonas aeruginosa*: Pathogenesis, virulence factors, antibiotic resistance, interaction with host, technology advances and emerging therapeutics. *Signal Transduction and Targeted Therapy*, 7(1): 199. <https://doi.org/10.1038/s41392-022-01056-1>
- [5] Hadab, M.A.K., Al-Nuaimi, B.N., Al-Asadi, A.B., Al-Maadhidi, J.F., Abdul-Gani M.N. (2020). Cytopathic effects of activated parasporal inclusion proteins produced from Iraqi isolates of *Bacillus thuringiensis*. *Annals of Tropical Medicine & Public Health*, 23(2): 190-199. <https://doi.org/10.36295/ASRO.2020.23226>
- [6] Pailhoriès, H., Herrmann, J.L., Velo-Suarez, L., Lamoureux, C., Beauruelle, C., Burgel, P.R., Héry-Arnaud, G. (2022). Antibiotic resistance in chronic respiratory diseases: From susceptibility testing to the resistome. *European Respiratory Review*, 31(164):

210259. <https://doi.org/10.1183/16000617.0259-2021>
- [7] Tooke, C.L., Hinchliffe, P., Bragginton, E.C., Colenso, C.K., Hirvonen, V.H.A., Takebayashi, Y., Spencer, J. (2019). β -Lactamases and β -Lactamase Inhibitors in the 21st Century. *Journal of Molecular Biology*, 431(18): 3472-3500. <https://doi.org/10.1016/j.jmb.2019.04.002>
- [8] Ingmer, H., Brøndsted, L. (2009). Proteases in bacterial pathogenesis. *Research in Microbiology*, 160(9): 704-710. <https://doi.org/10.1016/j.resmic.2009.08.017>
- [9] Al-Nuaimi, B.N., Al-Azzawi, R.H. (2024). Correlation between MicroRNA-155 expression and viral load in severe COVID-19 patients. *Journal of Communicable Diseases*, 56(4): 1-7. <https://doi.org/10.24321/0019.5138.202457>
- [10] Wang L.L., Hu, C., Shao, L. (2016). The antimicrobial activity of nanoparticles: Present situation and prospects for the future. *International Journal of Nanomedicine*, 12: 1227-1249. <https://doi.org/10.2147/IJN.S121956>
- [11] Mout, R., Moyano, D.F., Rana, S., Rotello, V.M. (2012). Surface functionalization of nanoparticles for nanomedicine. *Chemical Society Reviews*, 41(7): 2539-2544. <https://doi.org/10.1039/c2cs15294k>
- [12] Jadoun, S., Arif, R., Jangid, N.K., Meena, R.K. (2021). Green synthesis of nanoparticles using plant extracts: A review. *Environmental Chemistry Letters*, 19(1): 355-374. <https://doi.org/10.1007/s10311-020-01074-x>
- [13] Kirubakaran, D., Wahid, J.B.A., Karmegam, N., Jeevika, R., Sellapillai, L., Rajkumar, M., SenthilKumar, K.J. (2025). A comprehensive review on the green synthesis of nanoparticles: Advancements in biomedical and environmental applications. *Biomedical Materials & Devices*, 1-26. <https://doi.org/10.1007/s44174-025-00295-4>
- [14] Mohammed, S.H., Rheima, A.M., Al-aameri, D.A., Zaidan, H.K., Al-Sharify, Z.T. (2025). Impact of synthesized Zero-valence silver nanoparticles on acetylcholinesterase and xanthine oxidase: Toxicological and environmental implications. *Case Studies in Chemical and Environmental Engineering*, 11: 101095. <https://doi.org/10.1016/j.cesce.2025.101095>
- [15] Mirzaei, A., Esfahani, B.N., Ghanadian, M., Wagemans, J., Lavigne, R., Moghim, S. (2024). *Alhagi maurorum* extract in combination with lytic phage cocktails: A promising therapeutic approach against biofilms of multi-drug resistant *P. mirabilis*. *Frontiers in Pharmacology*, 15: 1483055. <https://doi.org/10.3389/fphar.2024.1483055>
- [16] Muhammad, G., Hussain, M.A., Anwar, F., Ashraf, M., Gilani, A.H. (2014). *Alhagi*: A plant genus rich in bioactives for pharmaceuticals. *Phytotherapy Research*, 29(1): 1-13. <https://doi.org/10.1002/ptr.5222>
- [17] Asghari, M.H., Fallah, M., Moloudizargari, M., Mehdikhani, F., Sepehrnia, P., Moradi, B. (2016). A systematic and mechanistic review on the phytopharmacological properties of *Alhagi* species. *Ancient Science of Life*, 36(2): 65-71. https://doi.org/10.4103/asl.ASL_37_16
- [18] de Lacerda Coriolano, D., de Souza, J.B., Bueno, E.V., Medeiros, S.M.F.R.D.S., Cavalcanti, I.D.L., Cavalcanti, I.M.F. (2021). Antibacterial and antibiofilm potential of silver nanoparticles against antibiotic-sensitive and multidrug-resistant *Pseudomonas aeruginosa* strains. *Brazilian Journal of Microbiology*, 52(1): 267-278. <https://doi.org/10.1007/s42770-020-00406-x>

- [19] Lee, C., Ventola, M.S. (2015). The antibiotics resistance crisis pharmacy and therapeutics. *Pharmacy & Therapeutics (P&T)*, 40: 277-283.
- [20] Wehr, H.M., Frank, J.H. (2004). Standard methods for the microbiological examination of dairy products (17th Edition). Washington, D.C.: The American Public Health Association. <https://doi.org/10.2105/9780875530024>
- [21] Aryal S. (2021). McFarland standards-principle, preparation, uses, limitations. *Microbe Notes*. <https://microbenotes.com/mcfarland-standards/>.
- [22] Sultana, B., Anwar, F., Ashraf, M. (2009). Effect of extraction solvent/technique on the antioxidant activity of selected medicinal plant extracts. *Molecules*, 14: 2167-2180. <https://doi.org/10.3390/molecules14062167>
- [23] Thakur, S., Sharma, S., Thakur, S., Rai, R. (2018). Green synthesis of copper nano-particles using *Asparagus adscendens* roxb. Root and leaf extract and their antimicrobial activities. *International Journal of Current Microbiology and Applied Sciences*, 7(4): 683-694. <https://doi.org/10.20546/ijemas.2018.704.077>
- [24] Sankar, R., Manikandan, P., Malarvizhi, V., Fathima, T., Shivashangari, K.S., Ravikumar, V. (2014). Green synthesis of colloidal copper oxide nanoparticles using Carica papaya and its application in photocatalytic dye degradation. *Spectrochimica Acta Part A: Molecular and Biomolecular Spectroscopy*, 121: 746-750. <https://doi.org/10.1016/j.saa.2013.12.020>
- [25] Chandraker, S.K., Lal, M., Ghosh, M.K., Tiwari, V., Ghorai, T.K., Shukla, R. (2020). Green synthesis of copper nanoparticles using leaf extract of Ageratum houstonianum Mill. and study of their photocatalytic and antibacterial activities. *Nano Express*, 1(1): 010033. <https://doi.org/10.1088/2632-959X/ab8e99>
- [26] Chang, D., Sharma, L., Dela Cruz, C.S., Zhang, D. (2021). Clinical epidemiology, risk factors, and control strategies of Klebsiella pneumoniae infection. *Frontiers in Microbiology*, 12: 750662. <https://doi.org/10.3389/fmicb.2021.750662>
- [27] Palusiak, A. (2022). Proteus mirabilis and Klebsiella pneumoniae as pathogens capable of causing co-infections and exhibiting similarities in their virulence factors. *Frontiers in Cellular and Infection Microbiology*, 12: 991657. <https://doi.org/10.3389/fcimb.2022.991657>
- [28] Singh, J., Kumar, V., Kim, K.H., Rawat, M. (2019). Biogenic synthesis of copper oxide nanoparticles using plant extract and its prodigious potential for photocatalytic degradation of dyes. *Environmental Research*, 177: 108569. <https://doi.org/10.1016/j.envres.2019.108569>
- [29] Thatyana, M., Dube, N.P., Kemboi, D., Manicum, A.L.E., Mokgalaka-Fleischmann, N.S., Tembu, J.V. (2023). Advances in phytonanotechnology: A plant-mediated green synthesis of metal nanoparticles using phyllanthus plant extracts and their antimicrobial and anticancer applications. *Nanomaterials*, 13(19): 2616. <https://doi.org/10.3390/nano13192616>
- [30] Dutta, A. (2017). Fourier transform infrared spectroscopy. In *Spectroscopic Methods for Nanomaterials Characterization*, 73-93. <https://doi.org/10.1016/B978-0-323-46140-5.00004-2>
- [31] Huston, M., DeBella, M., DiBella, M., Gupta, A. (2021). Green synthesis of nanomaterials. *Nanomaterials*, 11(8): 2130. <https://doi.org/10.3390/nano11082130>
- [32] Gupta, D., Boora, A., Thakur, A., Gupta, T.K. (2023). Green and sustainable synthesis of nanomaterials: Recent advancements and limitations. *Environmental Research*, 231: 116316. <https://doi.org/10.1016/j.envres.2023.116316>
- [33] Crisan, M.C., Teodora, M., Lucian, M. (2021). Copper nanoparticles: Synthesis and characterization, physiology, toxicity and antimicrobial applications. *Applied Sciences*, 12(1): 141. <https://doi.org/10.3390/app12010141>

NOMENCLATURE

| | |
|---------------------|---------------------------------------------------|
| MDR | Multidrug-resistant |
| Cu | Copper |
| CuONPs | Copper oxide nanoparticles |
| AH.CuONPs | <i>Alhagi maurorum</i> Copper oxide nanoparticles |
| FTIR | Fourier transform infrared analysis |
| XRD | X-ray diffraction |
| AFM | Atomic Force Microscopy |
| TEM | Transmission electron microscopy |
| <i>K. pneumonia</i> | <i>Klebsiella pneumonia</i> |
| <i>A. baumannii</i> | <i>Acinetobacter baumannii</i> |
| <i>P. mirabilis</i> | <i>Proteus mirabilis</i> |
| <i>P.aeruginosa</i> | <i>Pseudomonas aeruginosa</i> |